

Viscometer for low frequency, low shear rate measurements

Robert F. Berg and Michael R. Moldover

Thermophysics Division, National Bureau of Standards, Gaithersburg, Maryland 20899

(Received 17 February 1986; accepted for publication 10 April 1986)

We describe a torsion-oscillator viscometer whose low frequency (0.5 Hz) and very low shear rate (0.05 s^{-1}) are required for measurements of shear sensitive fluids such as microemulsions, polymer melts and solutions gels, and liquid mixtures near critical points. The viscometer has a resolution of 0.2% when used with liquid samples and a resolution of 0.4% when used with a dense gaseous sample. The viscometer operates under computer control and is compatible with submillikelvin temperature control.

INTRODUCTION

We describe a novel torsion-oscillator viscometer designed for accurate measurements of the shear viscosity at very low frequency (0.5 Hz) and very low shear rate (0.05 s^{-1}). The design is suited to precise studies of shear-sensitive fluids such as microemulsions, gels, polymer solutions and melts, colloidal solutions undergoing coagulation, and liquid mixtures near critical points.

The viscometer we describe is an example of a closed "cup" viscometer. The inertial element of the torsion oscillator (the cup or bob) is hollow and contains the entire sample within it. This results in a compact sample volume which is required to facilitate *in situ* mixing of multicomponent fluid mixtures, should they happen to undergo phase separation in the course of viscosity measurements. This viscometer can contain samples at pressures in excess of 10 MPa and has been used for viscosity studies of SF_6 near the gas-liquid critical point.

The present design was motivated primarily by the need to attain both a low frequency and a low shear rate during viscosity studies near critical points. Near the critical temperature T_c , the internal relaxation time τ of a fluid sample diverges as $|T - T_c|^{-1.8}$ and can reach 1 s in the experimentally accessible temperature range.¹ A viscosity measurement which violates the inequality $\omega\tau \ll 1$ (where ω is the angular frequency of the measurement) will encounter non-Newtonian viscoelastic behavior.² A measurement which violates the inequality $S\tau \ll 1$ (where S is the shear rate) will encounter a shift in the apparent critical temperature and non-Newtonian viscoelastic behavior.³

We note that other authors have reported designs of torsion-oscillator viscometers optimized for high unloaded Q (i.e., high mechanical quality factor, which is associated with high sensitivity) at low temperatures,⁴ high-accuracy studies of low-density pure gases,⁵ and the study of corrosive liquids at high temperatures.⁶ In the present work, we obtain the viscosity from measurements of the logarithmic decrement of an undriven torsion oscillator. In contrast, some authors have measured the oscillator amplitude at constant drive.⁷

Energy dissipation in torsion-oscillator viscometers

whose dimensions greatly exceed the viscous penetration depth $\delta = (2\eta/\rho\omega)^{1/2}$ is proportional to $(\eta\rho)^{1/2}$. (Here, η is the dynamic viscosity and ρ is the density.) In this work we assume that the density of fluid under study is known from other measurements. For a fluid with a density near 1 g/cm^3 , the present design is satisfactory for the range $200 \mu\text{poise} < \eta < 4 \text{ poise}$ (1 poise = 0.1 kg/m s). Within this range, the present instrument is an absolute one, i.e., the viscosity is determined from dimensional and time measurements; calibration with a standard fluid is not required.

The construction of the viscometer is described in Sec. I. The excitation and detection of the oscillator's motion is described in Sec. II and the reduction of the data is described in Sec. III. Section IV describes the current performance of the viscometer and Sec. V suggests improvements to the design.

I. CONSTRUCTION OF THE VISCOMETER

The construction of the viscometer will be described in three parts. First we shall describe the torsion bob, which contains the sample. Second, we shall describe the torsion fiber and its contribution to the oscillator decrement. Finally, the environment of the oscillator will be described.

A. Bob

Figure 1 shows the torsion oscillator as it hangs in the innermost shell of the thermostat. The inertial element of the oscillator is the bob, a hollow, thick-walled stainless-steel cylinder which contains the sample under study. In our prototype oscillator, the sample cavity within the bob was a right circular cylinder whose diameter and height are both 38 mm and whose walls are 4 mm thick. Cylindrical cavities are easy to manufacture. Moreover, an exact theory exists to calculate the dissipation within an oscillating cylinder, which is completely filled with a viscous fluid.⁸ The theory for a spherical cavity also exists.^{9,10} Thus a spherical cavity is a reasonable alternative to a cylinder. When we discuss the effects of a liquid-vapor meniscus within the cavity, it will become clear that a cavity consisting of a tall, thin cylinder atop either a sphere or a short, wide cylinder could be used to minimize the effects of the meniscus. Unfortunately, the exact flow field in such a cavity has not been obtained.

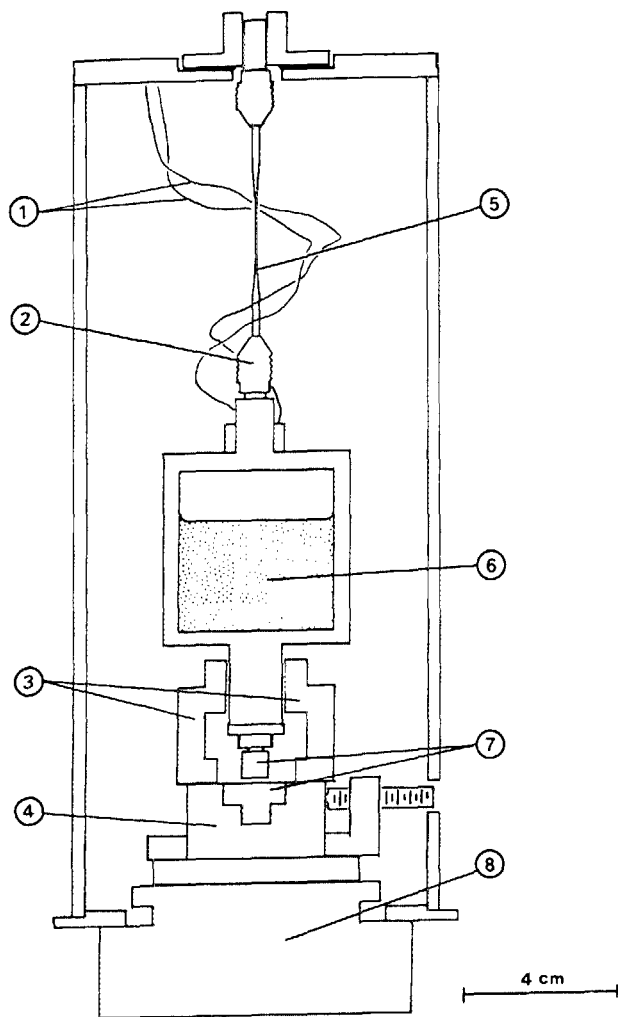


FIG. 1. The torsion oscillator hung inside the innermost thermostat shell. (1) Two of the five fine copper wires coiled into helices and used for electrical contact to the bob and its heater and thermistor. (2) Pin vise clamp to grip quartz rod. (3) Stationary electrode for excitation and detection of bob motion; the bob vane (seen edge-on) between the electrode surfaces forms the other half of a capacitor. (4) Translation stage for electrode positioning. (5) Torsion fiber drawn from 1-mm-diam quartz rod. (6) Liquid sample inside the cylindrical cup. (7) Rare earth magnet and copper disk used to reduce nontorsional oscillations. (8) Rotation stage for electrode positioning.

The lower portion of the bob has a complicated external shape because it serves three functions. It functions as an electrode, a valve, and a support for a magnet. Near the bottom of the bob, flats were milled in the cylindrical surface of the bob parallel to the torsion axis. Thus the bottom of the bob is a thick vane which is viewed end-on in Fig. 1. The vane is the moving electrode of a capacitor which is used to excite and detect the torsional motion of the bob. The vane also forms the body of the valve which is opened to load the sample. The valve is coaxial with the bob's torsional motion. The stem and packing of the valve were taken from a commercially manufactured, high-pressure stainless-steel "tee" valve. A hole 1.5 mm in diameter and 2.3 mm long leads from the valve to the cavity in the bob. Attached to the valve, at the very bottom of the bob, is a cylindrical rare-earth magnet. Its coaxial field is used to damp nontorsional motions.

A heater and a thermometer are mounted directly on the bob. The 500- Ω , thin-film, adhesive heater is wrapped on the outer surface of the bob. It can be used to change the temperature of the bob rapidly. Also, a heater power of a few watts has been used to convectively stir the sample between viscosity measurements when the sample strata are sufficiently close in density. For temperature measurement, we use a thermistor embedded with vacuum grease in an aluminum block at the top of the bob.

Electrical connections to the heater, thermistor, and bob itself (for the capacitance measurements) were made with five loosely coiled copper wires 90 μm in diameter.

A small, commercially manufactured, pin vise was soldered onto the top of the bob. The vise is used to attach the bob to the quartz torsion fiber. In order to avoid shattering the torsion fiber, it was necessary to sand 0.1-mm smooth flats onto the jaws of the vise with emery paper. A similar vise is used to fasten the other end of the fiber to the innermost shell of the thermostat.

We obtained the moment of inertia of the bob from measuring the changes in the period of the torsion oscillator which occurred when rings of calculable moment of inertia were placed on the bob.

B. Torsion fiber

Near or below ambient temperature, fused quartz is an excellent material for the torsion fiber. In contrast with most metals, fused quartz has very low internal losses and negligible creep. We have observed Q 's as high as 3×10^5 for a solid bob suspended from a quartz fiber.

The torsion fiber for the prototype oscillator was fabricated from a short, 1-mm-diam quartz rod. The middle of the rod was drawn to a diameter of about 0.3 mm over a length of 20 mm. The steps involved were (1) heat a 3-mm length of the rod to melting using a natural gas oxygen torch, (2) remove the flame, and (3) quickly stretch the rod (2 cm/1 s). The rod was held in a miniature drill press to facilitate control of this process. The 1-mm-diam ends of the rod were left intact for holding the fiber.

C. Environment

The accuracy and precision of the determination of the viscosity can be degraded by energy losses from the oscillator occurring outside the sample and from dissipation within the sample when fluid motions other than the desired axisymmetric oscillation occur. To control external dissipation, we have reduced the gas pressure outside the bob to less than 0.1 Pa and designed the electrical leads to the bob with care. Undesired fluid motions are minimized by three factors: (1) magnetically damping the pendulum and rocking motions of the bob, (2) taking modest precautions to isolate the oscillator from external vibrations, and (3) by ensuring that the temperature gradients across the bob are small enough to avoid convection during measurements.

1. Vacuum

In the presence of external gases, the oscillator's motion will be damped, especially by flow in the narrow gap between

the bob's vane and the stationary electrodes. A small mechanical vacuum pump is used to evacuate the entire thermostat prior to the measurements and then disconnected. Subsequently, a liquid-nitrogen-cooled sorption pump maintains the pressure below 0.1 Pa without introducing vibrations.

2. Vibrations

The thermostat and its two vacuum pumps rest on a 400-kg steel table supported by cork-rubber laminate pads. Most conventional vibration isolation tables are useless near the oscillator frequency (0.5 Hz). We have not established that the heavy table we used was in fact helpful. The unwanted pendulum and rocking motions induced in the bob were magnetically damped. To achieve this, a stationary, annealed, OFHC copper disk was fastened 1 mm below the cylindrical magnet attached to the bottom of the bob. This damping scheme is useful over a much wider temperature range than the needle and oil cup used elsewhere.^{9,11}

3. Connections to the bob

A heuristic argument guided the use of pin vises to clamp the fiber and the design of the electrical leads to the bob so as to minimize the mechanical losses due to these components. We assumed that the total elastic energy stored in the i th component when it is deflected through an angle θ_i is $E_i = k_i \theta_i^2 / 2$ and that the energy lost in that component $\Delta E_i = B_i E_i$. (Here k_i is a spring constant and B_i is a material-dependent loss factor.) The total Q of an oscillator assembled from many elastic components is given by the ratio

$$Q = 2\pi(\sum_i E_i) / (\sum_i \Delta E_i),$$

which, for parallel combinations of springs, is

$$Q = (\sum_i k_i) / (\sum_i B_i k_i)$$

and, for series combinations of springs, is

$$Q = (\sum_i k_i^{-1}) / (\sum_i B_i k_i^{-1}).$$

We have chosen a torsion fiber material with a low internal loss factor B_{fiber} . The effect of lossy components in parallel with the quartz fiber, such as the electrical leads, can be minimized by reducing their k_i . In this case thin wires shaped into large diameter, nontouching helices are used. The pin vises which grip the fiber are elastic elements in series with the torsion fiber. To minimize their effects, the fiber is gripped at the 1-mm-diam ends. This diameter is large compared with the drawn diameter so that the effect of B_{grip} is minimized by a large k_{grip} .

In practice, the oscillator with its leads connected has a Q near 3×10^4 when the bob is empty. This value is reproducible within $\pm 20\%$ and is very slightly (1%/K) dependent on temperature in the range 0–60 °C. When the bob is filled with water, the Q is reduced to roughly 300. Thus, there is no incentive to increase the empty Q , as long as measurements with an accuracy 0.4% are satisfactory.

D. Thermostat

The torsion oscillator, as shown in Fig. 1, hangs inside an aluminum shell. The temperature at one point on this

shell can be controlled to ± 0.05 mK. The vertical temperature difference along this shell $\Delta T(\text{shell})$ is monitored with a thermopile and nanovoltmeter. Differences of 1 mK can be reliably detected. Two additional aluminum shells are used but not shown. The outermost shell is a 15-cm-diam aluminum cylinder controlled to ± 50 mK which acts as the vacuum can for the thermostat. The most important heat transfer mechanism between the shells is radiation. The temperature of each shell is monitored with a thermistor and can be independently controlled.

Temperature gradients on the bob result from both the gradient imposed by the surrounding shell as well as the power required to maintain the bob at a temperature T_{bob} above the temperature of the surrounding shell T_{shell} . An estimate of these two contributions is

$$\Delta T_{\text{bob}} \simeq 0.01 \Delta T_{\text{shell}} + 0.02 (T_{\text{bob}} - T_{\text{shell}}).$$

Minimizing ΔT_{bob} requires that T_{shell} closely track T_{bob} .

An alternative to tracking is to simply turn off the bob heater and allow the bob to equilibrate with the shell. Because the time constant for this equilibration is about 3 h, exponential temperature sweeps can be implemented allowing T_{bob} to relax to T_{shell} over a period of many hours. During such a sweep a temperature gradient occurs within the sample. If convection is ignored, the temperature difference between the sample's center and its periphery is approximately $R^2 \dot{T} / (6D_T)$, where r is the sample's radius, \dot{T} is the cooling rate, and D_T is the sample's thermal diffusivity. This cooling-rate dependent gradient limits the maximum sweep rate at which reliable data can be obtained. During the sweeps, hundreds of decrement measurements are made and recorded along with T_{bob} , which is read by a digital ohmmeter to a precision of about 0.05 mK.

E. Electrodes

The stationary electrode used to excite and detect the bob's motion was designed to be sensitive to the torsional motion of the bob and insensitive to the pendulum motions of the bob. This electrode is comprised of two, 1-cm², flat, electrically connected surfaces. These surfaces face diametrically opposite sides of the vane. The stationary electrode was mounted on stacked commercially manufactured optical translation and rotation mounts. The mounts were used to position the electrode's surfaces 0.5 mm from the vane before closing the thermostat.

II. OSCILLATOR MOTION

The motion of the freely decaying torsion oscillator can be characterized by a maximum amplitude $\theta(0)$, an angular frequency ω , and a decrement D ,

$$\theta(t) = \theta(0) \sin(\omega t) e^{-D\omega t / 2\pi}, \quad (1)$$

where typically $\theta(0) \approx 1$ mrad. To observe the oscillator movement, the capacitance between the vane and the stationary electrode is measured using a commercial capacitance bridge and lock-in amplifier operating at 10 kHz and 5 V rms. This voltage produces a negligible perturbation on the oscillator's motion.

The output waveform from the lock-in amplifier is a damped sine wave distorted by the $1/x$ dependence of the capacitance on the electrodes' spacing x . We have chosen to obtain the decrement from measurements of the peak-to-peak voltage for which the $1/x$ distortion leads to a small, easily estimated, second-order correction. The peak voltages are measured with a digital voltmeter which is triggered $\frac{1}{4}$ period after each zero crossing.

The oscillator is excited by applying a sinusoidal voltage between the bob and the fixed electrode while the capacitance bridge is temporarily disconnected. Typically, three cycles at 60 V peak-to-peak at the oscillator's natural period are used. After starting the oscillations, we ignore five periods while short-lived transients in the fluid motion decay. We then measure 100 successive peak-to-peak voltages, from which the decrement is derived.

III. DATA REDUCTION

The theory derived by Newell and co-workers⁸ can be used to compute the viscosity from the measured decrement when the bob is completely filled with a homogeneous sample. The calculation requires the mass and density of the sample, the internal dimensions and moment of inertia of the bob, the period of the oscillator, and the decrement measured when the bob is empty. The calculation can be done very conveniently with an accuracy of 0.1% using a cubic "working equation."^{6,12} We note that the theory neglects phenomena which are quadratic in the amplitude of oscillation such as secondary flow and a parabolic curvature of the meniscus. We believe this is an excellent approximation for the present viscometer. For example, secondary flow about the exterior of an oscillating sphere of radius R is characterized¹³ by the dimensionless parameter $\theta_0^2 R^2 (\eta/\rho\omega)$. In our measurements this parameter is very small, roughly 10^{-4} .

The same theory of Newell and co-workers can be applied to the liquid-filled portion of a partially filled cylindrical bob, provided that the liquid-vapor surface intersects the cylindrical wall perpendicularly, i.e., with a contact angle of 90° , and that the vapor density is low. To obtain the liquid's viscosity in such a situation, one needs an estimate of the vapor's density and viscosity, and a crude model for the vapor's motion in addition to the data mentioned above.

In general, the contact angle is not 90° . Then one must estimate the contribution to the decrement from flow in the curved meniscus region. The meniscus contribution is roughly 5% of the total decrement when the bob is half full of water. This contribution depends upon both the contact angle and the capillary length. We have obtained independent, consistent estimates for the meniscus contribution to the decrement from auxiliary experiments and from a simple model. The experimental approach is to carry out two measurements of the decrement, each with a different filling of the bob, typically, $\frac{1}{3}$ and $\frac{2}{3}$ full. To an excellent approximation, the difference between the $\frac{1}{3}$ -full decrement and $\frac{2}{3}$ -full decrement can be attributed to a virtual, meniscus-free, sample of the liquid whose height is $\frac{1}{3}$ of the height of the cavity in the bob. This approximation is not exact (even when the viscous penetration length is small compared with the sample height) because the oscillator's period changes with the

filling.

The model calculation we use to estimate the dissipation in the meniscus region is based on the dissipation per unit area $P(x)$ of an infinite oscillating plane¹⁰ covered with a fluid layer of thickness x . We numerically compute a length h_0 to be added to the liquid's height, where

$$h_0 = \int_0^a P[x(z)] dz / P(\infty). \quad (2)$$

Here $x(z)$ is the meniscus profile as a function¹⁴ of the height z and the integration limit a is the capillary length. The value of the viscosity used in $P(x)$ is estimated from the "working equation" neglecting the meniscus contribution. The h_0 is added to the height h of the liquid in the central portion of the sample and the viscosity is recalculated.

In the data reduction, h is computed from the volume of the bob, the weight and density of the sample, and the volume occupied by the curved part of the meniscus. We allow for the thermal expansion of the bob and the liquid.

IV. PERFORMANCE

Here we discuss the precision and accuracy of the viscometer and we display the results of measurements on three different fluids.

The precision (not the absolute accuracy) of the viscosity measurements is about $\pm 0.2\%$ for water or a similar liquid. When a gas sample is studied, both the viscosity and the density are lower. Thus, the measured decrement is lower and more sensitive to externally induced vibrations of the bob. The precision of the viscometer is $\pm 0.4\%$ when filled with SF_6 near its liquid-vapor critical point. We believe the precision is limited by vibrations of the bob, not by electronic noise in the measurements of the bob's motion.

As a check on the absolute accuracy of our viscometer, we measured the viscosity of water over the range of 30 – 60°C . Because water need not perfectly wet the container walls, the meniscus correction had a free parameter (the contact angle). By setting the contact angle to zero, both data sets ($\frac{1}{3}$ and $\frac{2}{3}$ full) agreed with each other within their scatter. The data differed from the accepted viscosity of water¹⁵ by at most 0.8%. The accuracy of the measurements is limited by imperfect knowledge of the meniscus effects and imperfect knowledge of the decrement of the empty oscillator.

Figure 2 shows data spanning two decades in viscosity. The highest viscosity curve represents data for a microemulsion comprised of decane, water, and the surfactant AOT. These data display the strong increase in viscosity near the lower critical solution temperature of the microemulsion at 35°C . The lowest viscosity curve in Fig. 2 represents data for SF_6 at its critical density taken just above the liquid-vapor critical temperature, $T_c = 45^\circ\text{C}$. Figure 2 also displays two sets of data for a mixture of methanol and cyclohexane near its critical composition under two different conditions described below.

In Fig. 3 the logarithm of the viscosity is plotted as a function of the logarithm of $|T - T_c|$. Figure 3 emphasizes the viscosity anomaly at the consolute point of a methanol-cyclohexane mixture. Previous measurements of compara-

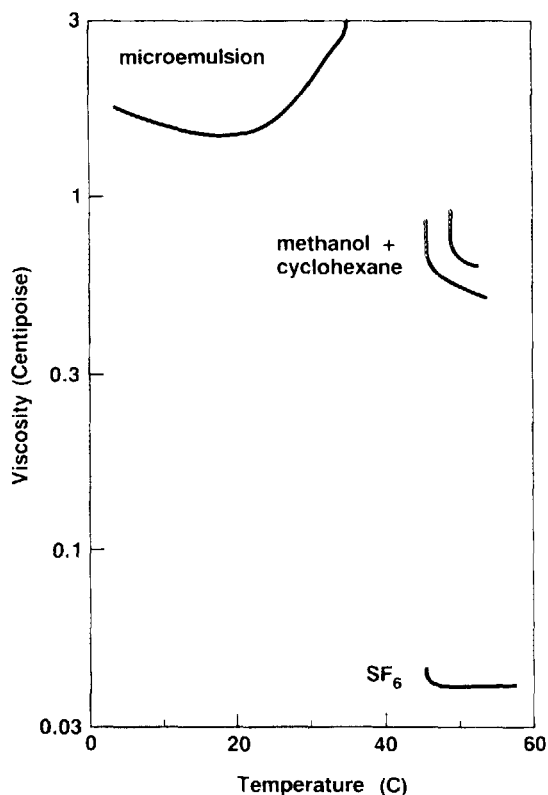


FIG. 2. Four examples of critical viscosity measurements on three samples with rather different viscosity ranges and pressures. One set of the methanol + cyclohexane data was taken at vapor pressure and the other at essentially constant density.

ble viscosity anomalies have, in effect, less temperature resolution because they violated either the inequality $\omega\tau < 1$ or the inequality $S\tau < 1$.

In Fig. 3, the lowest band of points are methanol-cyclohexane data from two runs at 1/3 full and two runs at 2/3 full. The four runs are indistinguishable on the figure, indicating the excellent consistency of the data. To reduce these data, we assumed the contact angle between the mixture and the viscometer's wall was zero and we used the model calculation, Eq. (2). An additional run at 1/7 full is not shown; however, it was consistent with the others to within 1% in the range $10^{-4} < (T - T_c)/T_c < 10^{-2}$. A more detailed discussion of these data and deviation plots from fitted power laws are given elsewhere.¹¹

The upper band of points on Fig. 3 contains data from three runs where the bob was completely filled with the methanol-cyclohexane mixture at temperatures above 37°C. Near T_c the pressure for these runs is above 11 MPa and the density is roughly 1% higher than the density at the vapor pressure. This 1% increase of the sample's density causes an 8% increase in the viscosity at the same value of $(T - T_c)$. These data illustrate viscosity measurements approaching T_c on two different thermodynamic paths, at saturated vapor pressure and at constant volume.

V. POSSIBLE IMPROVEMENTS

Presently, our viscometer performs satisfactorily in the 0–60°C temperature range. We plan to extend this range

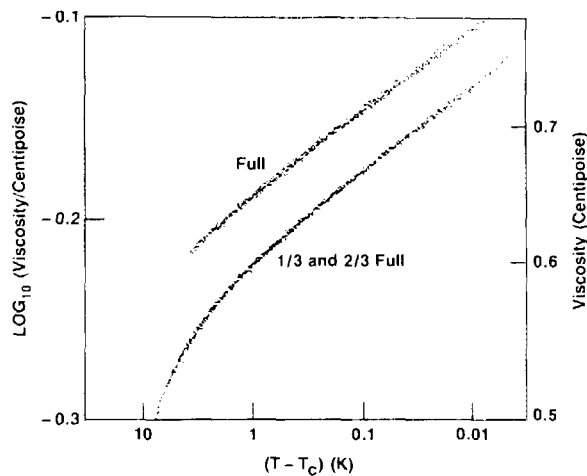


FIG. 3. Methanol + cyclohexane viscosity vs $T - T_c$. The three runs for the full loading have higher viscosities due to their high sample pressures (≈ 10 MPa). The consistency of the four runs for the partial cup loadings support the validity of the model used for the meniscus correction.

down to at least -50°C by circulating cold gas in the middle thermostat shell. We have also designed a much smaller bob whose smaller thermal time constants should facilitate more rapid acquisition of data. For routine measurements with liquid samples at saturated vapor pressure, we are experimenting with a bob designed to reduce the effects of the meniscus. In this bob, the sample cavity is a sphere with a tall, thin cylinder atop it. Over a reasonable range of temperatures, the meniscus will be in the cylindrical portion of the cavity, where its contribution to the decrement will be small. We believe that improved vibration isolation will lead to improved resolution of the viscosity measurements.

ACKNOWLEDGMENTS

We are happy to acknowledge continuing advice and encouragement from R. W. Gammon, F. Guzman, E. A. Kearsley, J. Kestin, and G. G. Luthor. This work has been supported in part by the Microgravity Sciences Program of NASA under contract C-86129D.

¹M. R. Moldover, in *Opportunities for Academic Research in a Low-Gravity Environment*, edited by G. Hazelrigg and J. Reynolds (AIAA, New York, 1986); Critical viscosity measurements are reviewed by J. V. Sengers, *Int. J. Thermophys.* **6**, 203 (1985).

²J. K. Bhattacharjee and R. A. Ferrell, *Phys. Rev. A* **27**, 1544 (1983).

³D. W. Oxtoby, *J. Chem. Phys.* **62**, 1463 (1975); A. Onuki, Y. Yamazaki, and K. Kawasaki, *Ann. Phys.* **131**, 217 (1981); D. Beysens, M. Gbadamassi, and B. Moncef-Bouanz, *Phys. Rev. A* **28**, 2481 (1983).

⁴R. N. Kleiman, G. K. Kaminsky, J. D. Reppy, R. Pindak, and D. J. Bishop, *Rev. Sci. Instrum.* **56**, 2088 (1985).

⁵A review of large-amplitude, low-frequency torsional oscillator viscometers is by J. Kestin, *Phys. Chem. Earth* **13–14**, 295 (1982).

⁶W. Brockner, K. Tørklep, and H. A. Øye, *Ber. Bunsenges Phys. Chem.* **83**, 1 (1979).

⁷R. N. Kleiman, D. J. Bishop, R. Pindak, and P. Taborek, *Phys. Rev. Lett.* **53**, 2137 (1984).

⁸J. Kestin and G. F. Newell, *Z. Angew. Math. Phys.* **8**, 433 (1957); D. A. Beckwith and G. F. Newell, *ibid.* **8**, 450 (1957).

⁹E. A. Kearsley, *Trans. Soc. Rheol.* **3**, 69 (1959); H. S. White and E. A. Kearsley, *J. Res. NBS* **75A**, 541 (1971).

¹⁰L. D. Landau and E. M. Lifshitz, *Fluid Mechanics* (Pergamon, New York, 1954), Sec. 24.

¹¹R. F. Berg and M. R. Moldover, *Int. J. Thermophys.* (in press).

¹²J. M. Grouvel and J. Kestin, *Appl. Sci. Res.* **34**, 427 (1978).

¹³R. C. DiPrima and N. Liron, *Phys. Fluids* **19**, 1450 (1976).

¹⁴L. D. Landau and E. M. Lifshitz, *Fluid Mechanics* (Pergamon, New

York, 1954), Sec. 60.

¹⁵The four-parameter equation of J. F. Swindells, in *Handbook of Chemistry and Physics*, edited by R. C. Weast (CRC Press, Cleveland, 1974) is sufficiently accurate (0.1%) over the range 30–60°C when compared with more recent representations: see J. V. Sengers and B. Kamgar-Parsi, *J. Phys. Chem. Ref. Data* **13**, 185 (1984).